JOURNAL OF SOLID STATE CHEMISTRY **121,** 262–272 (1996)
ARTICLE NO. 0037

$Tl_2Ba_2CaCu_2O_8$ Superconducting Thin Films: A Comparative Study of *ex Situ* Annealing Using Amorphous Precursors with Different Thallium Content

C. Gasser, A. Taffin, B. Mercey, F. Studer, and H. Murray

Laboratoire de Cristallographie et Sciences des Matériaux, Institut des Sciences de la Matière et du Rayonnement, Université de Caen, Boulevard Maréchal Juin, 14050 Caen Cedex, France

and

P. Berger

Laboratoire Pierre Sue CEN Saclay, Saclay, France

Received May 15, 1995; in revised form September 18, 1995; accepted September 19, 1995

The synthesis of $Tl_2Ba_2CaCu_2O_8$ (2212) films obtained by *ex situ* annealing of amorphous films, deposited at room temperature with a multitarget sputtering system, is described. The growth phenomenon of 2212 films has been extensively studied by annealing precursor thin films of variable thallium content under various O_2 partial pressures. The best single-phase 2212 films are obtained from stoichiometric amorphous precursor films. Such 2212 films, annealed under low oxygen pressure, exhibit a critical temperature for superconductivity T_c (Resistivity = 0) at 110 K with a critical current density J_c (77 K) $> 10^6 A/cm^2$. After annealing, the composition of these films, deduced from the backscattering spectra of $^4He^+$ beam measurements, indicates a formula close to Tl : Ba : Ca : Cu = 2 : 2 : 1 : 2.

INTRODUCTION

Since the discovery of superconductivity in thallium cuprates (1), several groups have performed the synthesis of thin films of these materials which turn out to be good candidates for active and passive low-temperature microelectronic devices (2). Thin films have been prepared by laser ablation (3), monotarget and multitarget sputtering (4–5), thermal evaporation (6), and MOCVD (7). The *in situ* method of preparation (8) of Tl based cuprate thin films has not allowed high T_c to be achieved because of the high volatility of thallium oxide. All attempts to synthesize such thin films can be divided into two methods (9) which are essentially characterized by the difference in thallium composition of the precursor films:

(i) One-step method. An amorphous precursor film containing thallium is prepared, and then annealed under oxygen with a pellet of $Tl_2Ba_2CaCu_2O_8$ unreacted material to provide the crystallized films with the right oxygen and thallium concentration, thus ensuring a good superconducting behavior.

(ii) Two-step method. An amorphous thallium-free precursor film is prepared, and then annealed under oxygen with a pellet of $Tl_2Ba_2CaCu_2O_8$ unreacted material. In this synthesis, thallium must be incorporated into the film during the annealing process. A precise adjustment of the annealing conditions is necessary to induce a good superconducting behavior in the crystallized film.

Heating the precursor films in vacuum sealed quartz tubes or in tube furnaces under an oxygen pressure has been reported. Although thallium-based cuprate superconductors exhibit superconducting transitions up to 120 K, the rapid loss of thallium by volatilization of thallium oxide during annealing represents one of the main difficulties for obtaining pure phases from a precursor film. In a previous paper, Lanham *et al.* (10) reported the phase evolution of thallium cuprate films as a function of annealing time, using an amorphous precursor film with a composition Tl : Ba : Ca : Cu = 6.2 : 2 : 1.5 : 3.5. The conclusion of this work is that 2212 films are formed from a decomposition of the precursor film with Tl_2O loss. More recently, W. L. Holstein (11) published an exhaustive review of thermodynamic data for different thallium oxides and concluded that an understanding of vapor phase processing is necessary to optimize the growth of Tl-based superconductors. We present in this paper, the phase changes of $Tl_xBa_2CaCu_2O_y$ precursor films during annealing in a sealed quartz tube and in a high oxygen pressure furnace. The second annealing method is used to show the different phases formed as a function of time.

0022-4596/96 $18.00

TABLE 1
Experimental Deposition Conditions for the Cuprate Precursor

Gas	Pressure (mbar)
Argon	10^{-2}
Oxygen	10^{-3}
Targets	Voltage (V)
Ca_2CuO_3	500
$Ba_{1.8}Ca_{0.2}CuO_3$	700
Thallium	0–900
Copper	300

EXPERIMENTAL

Deposition

In a previous paper (12), we described our multitarget sputtering system that allows a homogeneous deposition over an area 5 cm in diameter and also allows, by a special choice of specific targets, the preparation of several compositions in the Tl-based superconductor system. A brief description of the sputtering system follows.

First, four cathodes are mounted in the sputtering chamber. Two of these cathodes are fitted with insulating targets ($Ba_{1.8}Ca_{0.2}CuO_3$ and Ca_2CuO_3) and are R.F. biased (with self-dc voltage between 500 and 1000 V). The other two cathodes are fitted with metallic targets (Tl, Cu) and are dc biased. The substrate holder rotates with a low rotation speed (10 rpm) and sequentially faces the four targets.

This four target system is particularly suitable for the preparation of precursor films having different thallium compositions. All films have been deposited without intentional heating of the substrate (Table 1). The deposition time is 12 h in order to obtain 3000 Å thickness. As-deposited films are insulting and amorphous. Tl : Ba : Ca : Cu = 2 : 2 : 1 : 2 amorphous precursor films are relatively stable in air and can be annealed even after several days. Conversely, $Ba_2CaCu_2O_5$ precursors films react very quickly in air (between 5 and 10 min) to form barium and calcium carbonates.

Annealings

Three types of annealing treatments were performed on these films:

—sealed tube under low oxygen pressure (1 bar of oxygen),

—sealed tube under intermediate oxygen pressure (10 bar of oxygen),

—annealing under high oxygen pressure (70 bar of oxygen).

During all these treatments, the films deposited on single crystalline $LaAlO_3$ (100) oriented substrates were wrapped in gold foil together with a Tl : Ba : Ca : Cu = 2 : 2 : 1 : 2 pellet of unreacted materials in order to provide a thallium oxide pressure near the film. The oxygen pressure was estimated by the decomposition in BaO and O_2 of BaO_2 in the pellet for low oxygen pressure annealing and by the reaction $BaO_2 + Tl_2O_3 \rightarrow Ba_2Tl_2O_5 + O_2$ which takes place in a crucible placed in the tube for the medium oxygen pressure annealing. Consequently, these values give only an order of magnitude and must be handled carefully. The annealing parameters are summarized in Table 2.

Post-Annealings

In order to increase T_c, post-annealing treatments may be applied to the films. In this case, films are heated up to 180°C in an argon or hydrogen/argon (10% of hydrogen) flow for 5 to 15 min.

Patterning

After complete annealing, the films are very stable in air and can be patterned by wet etching with EDTA for further application. The microbridge obtained is 15-μm wide, 5000-Å thick, and 1-mm long.

Characterization

After patterning, the films can be characterized electrically by resistivity measurement, using the four probe method in the ac mode with a criteria of 1 μV/cm. The measurements were made by a group working on components and the method was completely described elsewhere

TABLE 2
The Three Types of Annealing Conditions of Cuprate Films

	Sealed quartz tube	Sealed quartz tube	Furnace with O_2
Pressure of oxygen (bar)	1	10	70
Temperature slope (°C/min)	8.5	8.5	3
Dwell temperature (°C)	850	870	880
Duration	10 (min)	10 (min)	15 (h)

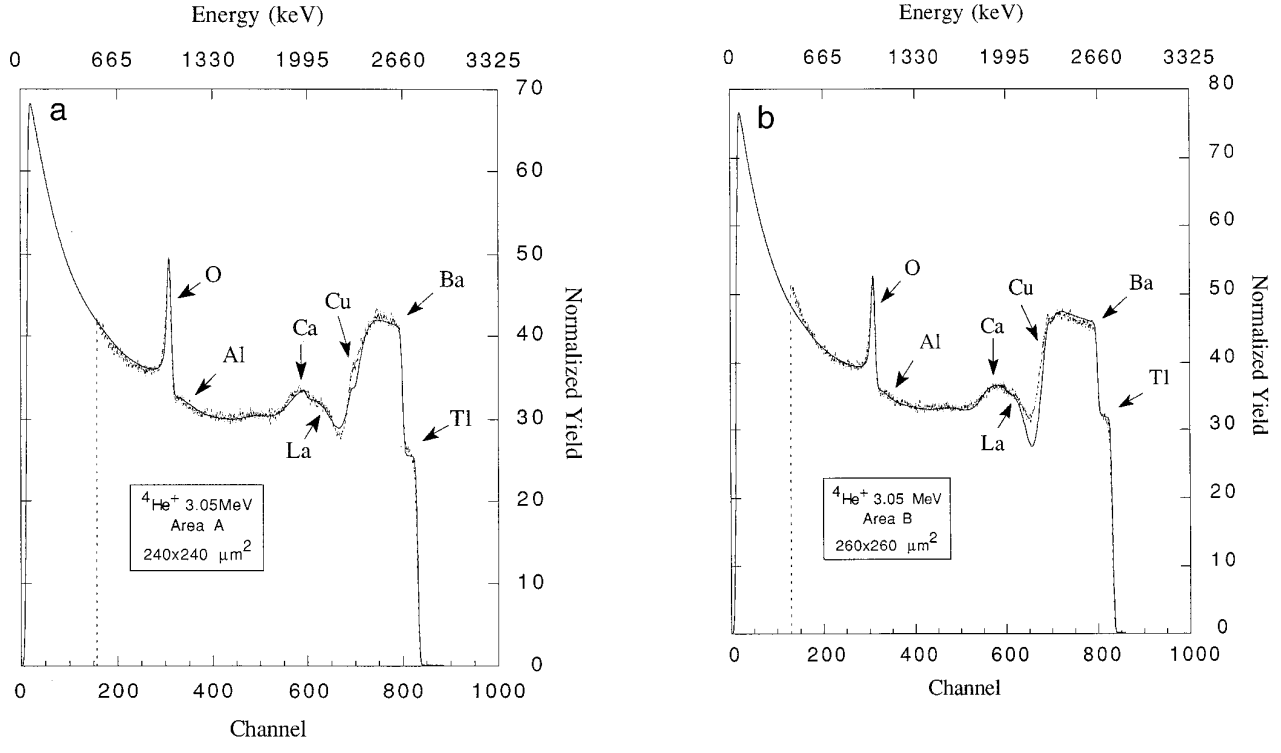

FIG. 1. Rutherford backscattering response of a 2212 thin film irradiated by $^4He^+$ beam for area A (a) and area B (b).

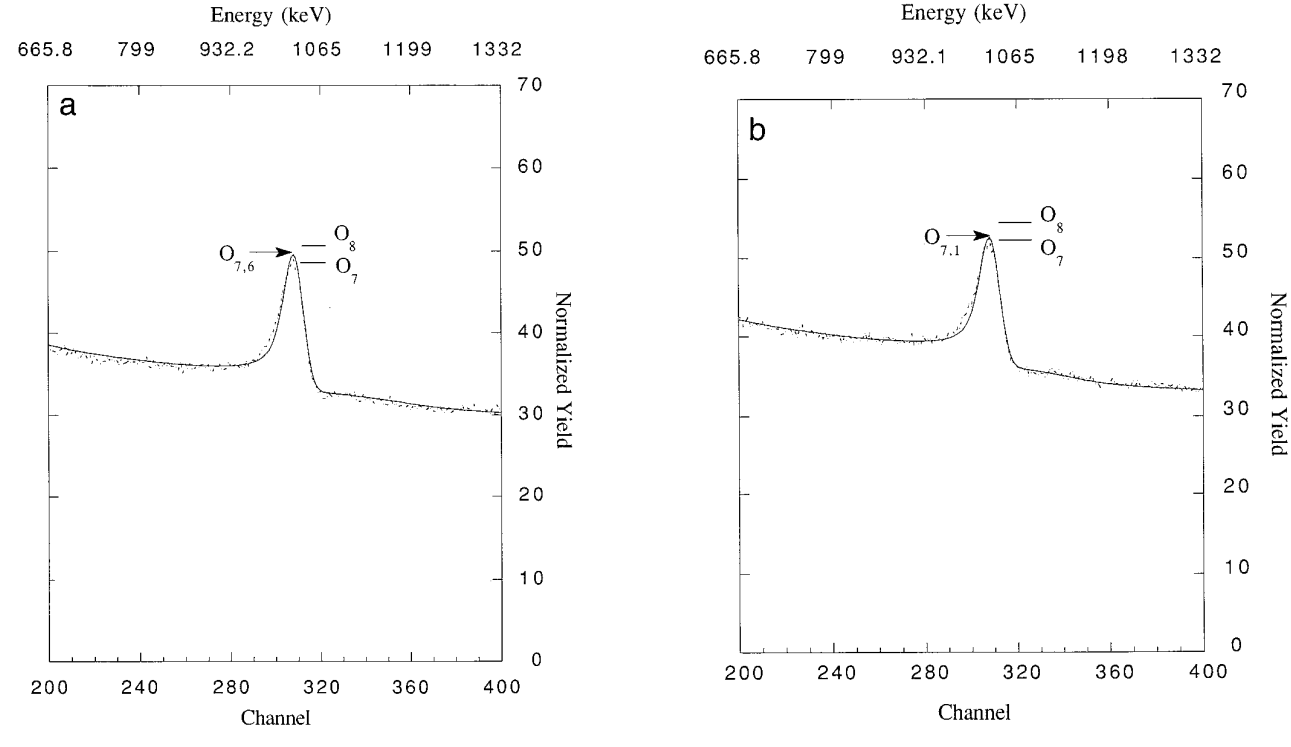

FIG. 2. Measurement of the film oxygen content for area A (a) and area B (b).

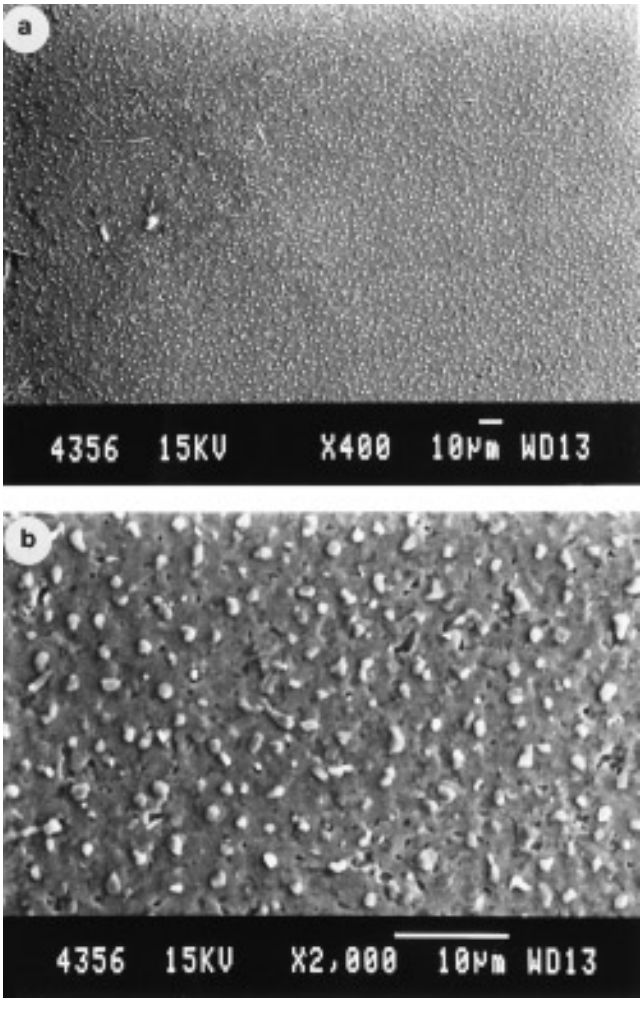

FIG. 3. Scanning electron microscope pictures of a film annealed in a sealed quartz tube under low oxygen pressure at an original magnification of (a) ×400 and (b) ×2000.

(13). Magnetic susceptibility measurements (ac) have been performed at a frequency of 80 Hz with a magnetic field of 1 G on a Lake Shore susceptometer. The field was oriented perpendicular to the film. A scanning electron microscope (SEM) fitted with a TRACOR analytical system working in the energy dispersive spectroscopy mode (EDS) was used to observe the surface of the film and also to determine the composition of the film before and after annealing. A Jeol 200CX transmission electron microscope (TEM) fitted with an eucentric goniometer ±60° and a Kevex EDS analytical system was used to perform precise determination of the microstructure of the film. Samples used for the TEM studies were prepared using the standard methods to obtain the plane and cross section (14).

Ion beam measurements were made on the 4 MeV Van de Graff accelerator of the nuclear studies center of BORDEAUX/GRADIGNAN (CENBG). A 3.05 MeV beam of $^4He^+$ was used with a classical backscattering setup (see Fig. 1). The RUMP program package (15) has been used for data reduction of the backscattering spectra. Standard cross section files were used for oxygen resonance handling.

RESULTS

Film Composition

The composition of the 2212 films, especially the oxygen content, was determined by comparison between experimental and simulated spectra of backscattered ^4He. Due to the roughness of the surface for this type of annealing, thickness deviation within the scanned area induces poorly resolved signals for copper and calcium edges. Tl/Ba ratios can be determined without ambiguity, but the relative accuracies on copper and calcium contents cannot be better

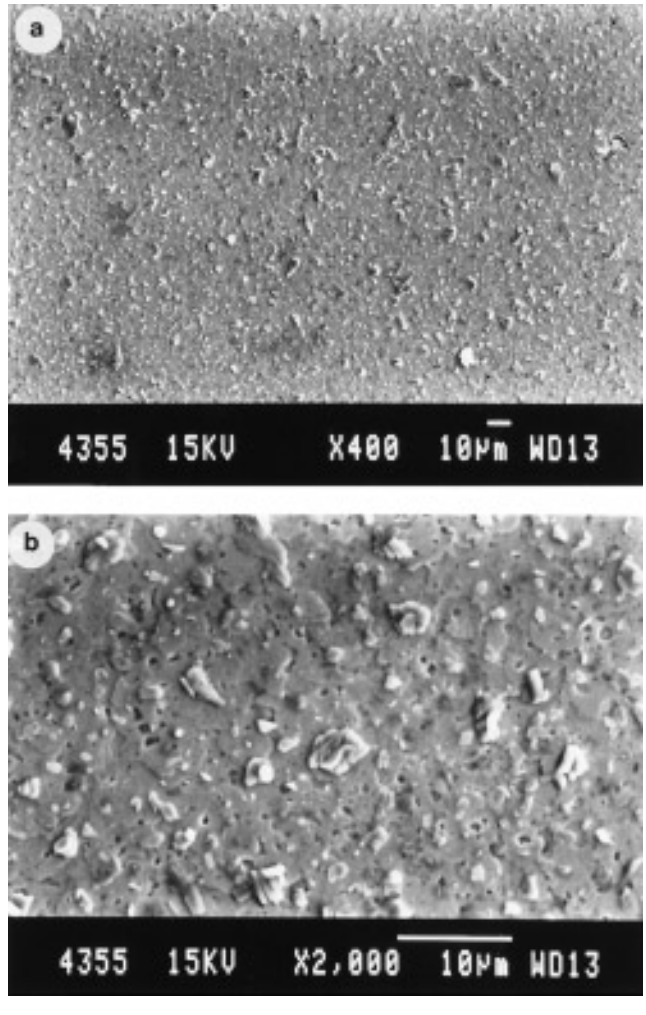

FIG. 4. SEM pictures of a film annealed in a sealed quartz tube under medium oxygen pressure at an original magnification of (a) ×400 and (b) ×2000.

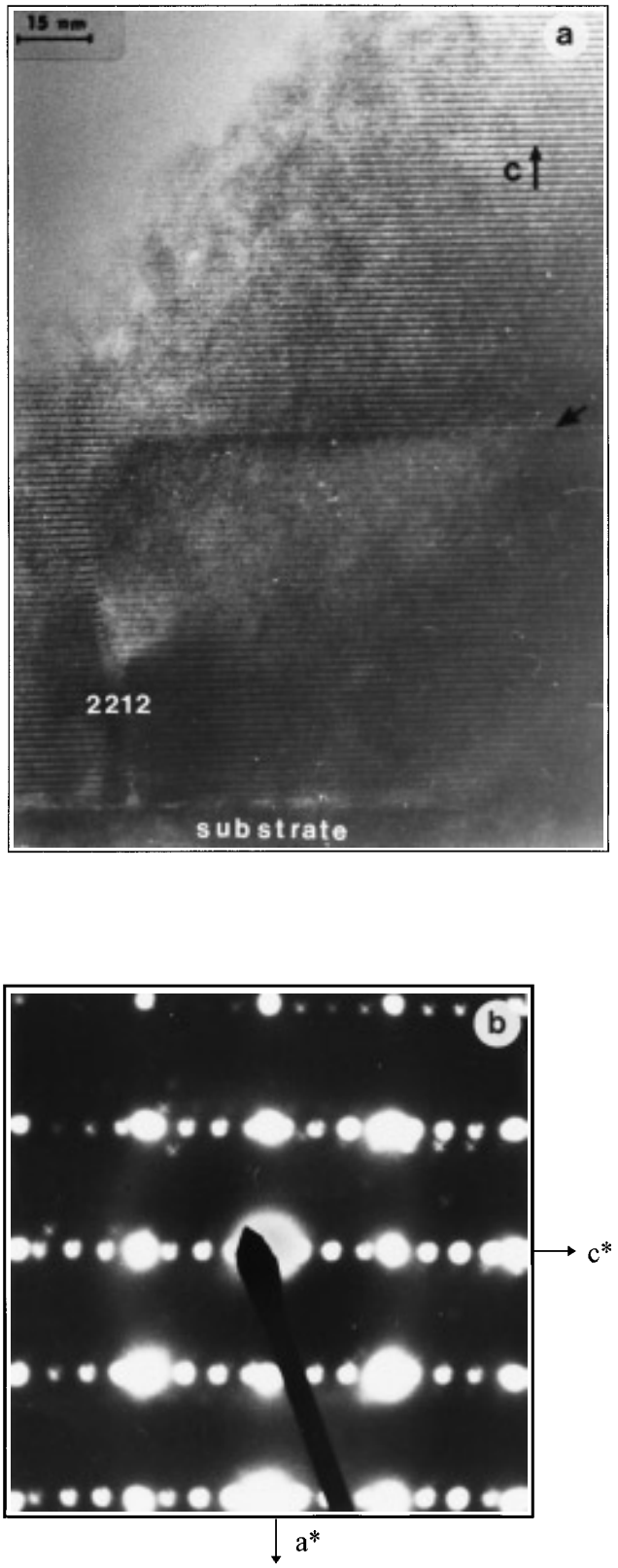

FIG. 5. Cross-sectional picture (a) made by a TEM of a film annealed in a sealed quartz tube under low oxygen pressure and the corresponding diffraction pattern (b).

than 10 and 20%, respectively. The oxygen stoichiometry is measured by means of the 3.045 MeV resonance. For a given stoichiometry, the relative accuracy is 5% (cf. Figs. 2a, 2b).

The backscattering spectra can be simulated from compositions $Tl_{1.6}Ba_{2.0}Ca_{1.2}Cu_2O_{7.6}$ (area A) and $Tl_{1.7}Ba_{1.7}Ca_{0.8}Cu_2O_{7.1}$ (area B). Taking a reference density of 7 g/cm^3 for the 2212 compound, the determined thickness for areas (A) and (B) are 640 ± 70 and 745 ± 53 nm, respectively. Although the fitting of the oxygen signal depends on the cation stoichiometry, the resulting composition always shows a fully oxygenated sample. As the oxygen resonance is rather narrow (10 keV), the analyzed depth is limited to approximately the top 200 nm of the layer.

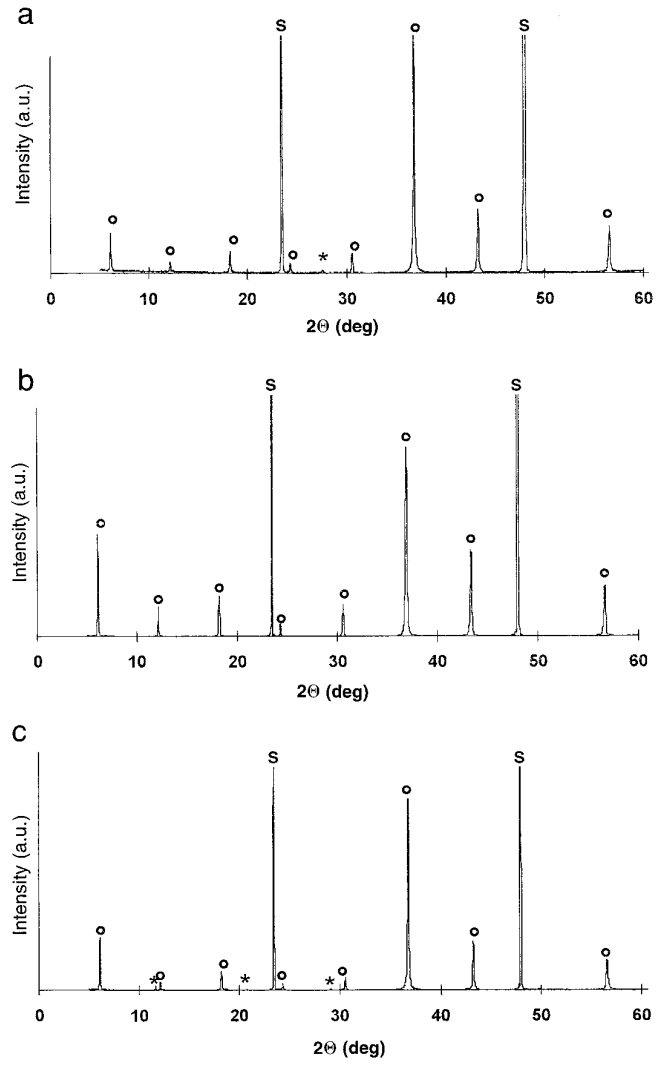

FIG. 6. X-ray diffraction pattern of films made by annealing in a sealed quartz tube with a Tl : Ba : Ca : Cu = 2 : 2 : 1 : 2 precursor film under low oxygen pressure (a), medium oxygen pressure (b), and a film made with a Tl : Ba : Ca : Cu = 0 : 2 : 1 : 2 precursor film under low oxygen pressure (c).

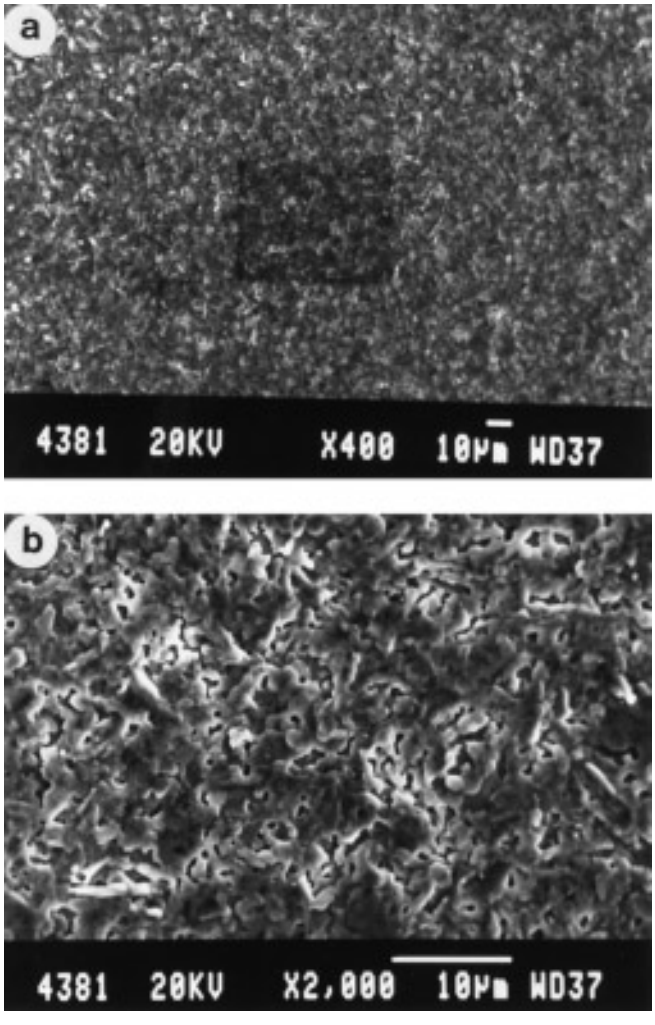

FIG. 7. SEM picture of a 0212 precursor film annealed under low oxygen pressure at an original magnification of (a) ×400 and (b) ×2000.

Annealing in a Sealed Quartz Tube

Tl : Ba : Ca : Cu = 2 : 2 : 1 : 2 precursor films. Films were annealed in a sealed quartz tube with low or medium oxygen pressure. In both cases, the short duration of annealing does not allow a study of the phase evolution. After 10 min, films were cooled to room temperature. In the case of low oxygen pressure annealing (1 bar), the SEM images (Fig. 3a) indicate a well-crystallized and uniform film. Insulating particles can be seen everywhere on the surface of the film. With a higher magnification (Fig. 3b), it is possible to observe that the film is almost nonporous. The T_c is about 105 K and a critical current density J_c (77 K) $> 10^6 A/cm^2$. For the medium oxygen pressure annealed films (20 bar), the surface also appears well crystallized (Fig. 4a). Large insulating particles are still visible on the surface. At a higher magnification (Fig. 4b) it is easy to see that the surface exhibits less particles than in the case of low oxygen pressure annealing. For the films annealed in medium oxygen pressure, the T_c is about 100 K.

As reported earlier (16), the high quality of the film grown on $LaAlO_3$ can be seen by electron microscopy (Fig. 5a). In this picture, a cross section from a low pressure annealed film is shown. The only defect (black arrowed) observed in the perfect stacking of the 2212 layers, attested by the regularity of the fringes, is the existence of a 2201 layer, that induces a stacking fault and an associated dislocation. The corresponding diffraction pattern (Fig. 5b) indicates that the film is perfectly oriented with respect to the substrate; that is, no rotation between the two diffraction patterns (film and substrate) is measurable.

Tl : Ba : Ca : Cu = 0 : 2 : 1 : 2 precursor films. Tl : Ba : Ca : Cu = 0 : 2 : 1 : 2 presursor films were annealed in the same way as Tl : Ba : Ca : Cu = 2 : 2 : 1 : 2 films. As reported above, such films must be rapidly placed in a vacuum sealed quartz tube after deposition to avoid forma-

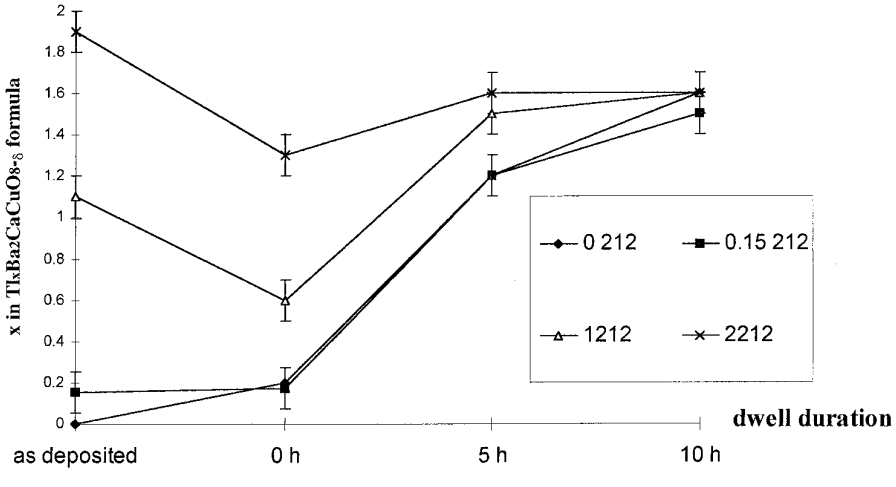

FIG. 8. Tl content variation versus annealing time for various X212 precursor films.

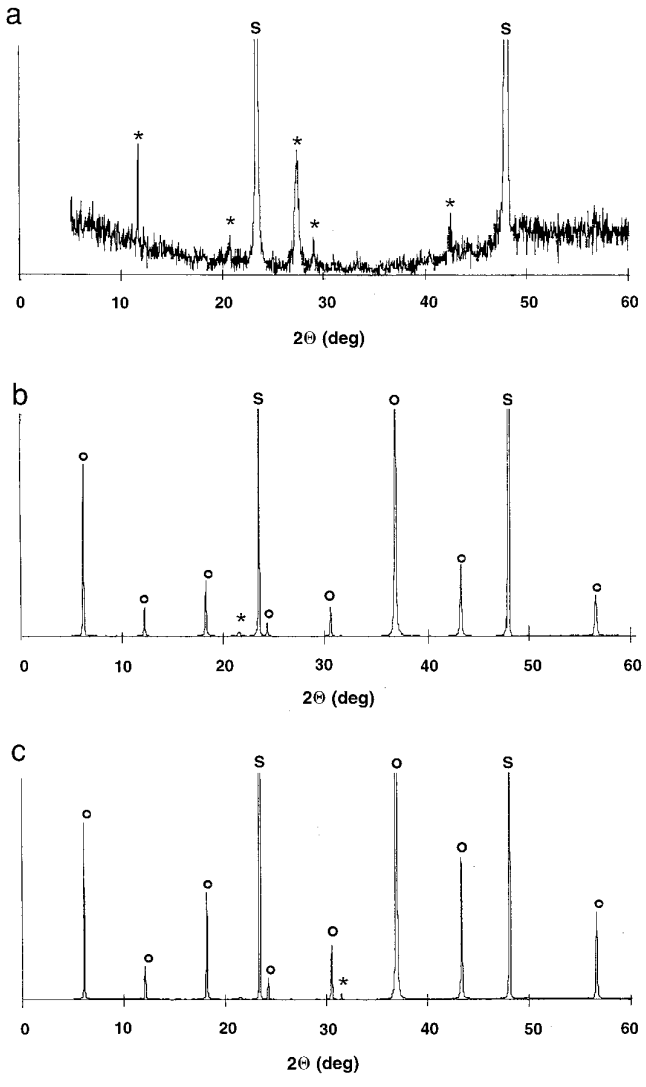

FIG. 9. X-ray diffraction pattern for various annealing times of 0212 precursor film. (a) 0 h, (b) 5 h, (c) 10 h ((S) substrate peaks, (o) 2212 phase (*) unknown phase).

tion of barium and calcium carbonates. After 10 min annealing, the films were cooled to room temperature for structural analysis. Films grown from Tl:Ba:Ca:Cu = 2:2:1:2 or 0:2:1:2 precursors do not exhibit significant differences between final phases after such annealing. The final composition of an annealed film, from a Tl:Ba:Ca:Cu = 0:2:1:2 precursor, is close to that obtained after annealing from a Tl:Ba:Ca:Cu = 2:2:1:2 precursor, and the X-ray diffraction pattern shows the presence of other phases in both cases (Figs. 6a and 6c). For a film synthesized under medium oxygen pressure there are no other phases visible (Fig. 6b). The other difference between the films grown from the two different precursors arises from the surface morphology of the film. The best final surface morphology is detained from the Tl:Ba:Ca:Cu = 2:2:1:2 precursor (Figs. 7a and 7b). It is clear that for further applications, such as etching and deposition, these differences are very important. Films from Tl:Ba:Ca:Cu = 2:2:1:2 precursors do not exhibit surface defects after annealing and are easier to etch.

Annealing in a High Oxygen Pressure

This annealing process is well suited for studying the crystallization. The slow crystallization rate allows one to stop the process at different annealing times.

Precursor films with different thallium content Tl:Ba:Ca:Cu = X:2:1:2. Annealing in a high oxygen pressure induces also the formation of the 2212 phase after several hours. This technique is thus particularly well-

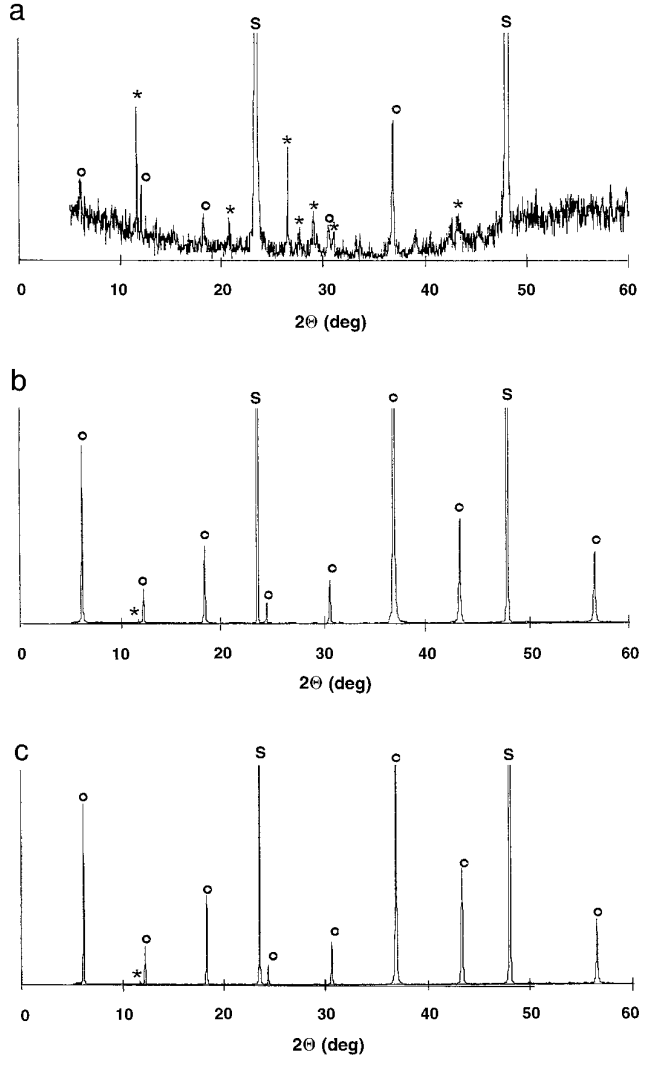

FIG. 10. X-ray diffraction pattern for various annealing times of 1212 precursor film. (a) 0 h, (b) 5 h, (c) 10 h ((S) substrate peaks, (o) 2212 phase, (*) unknown phase).

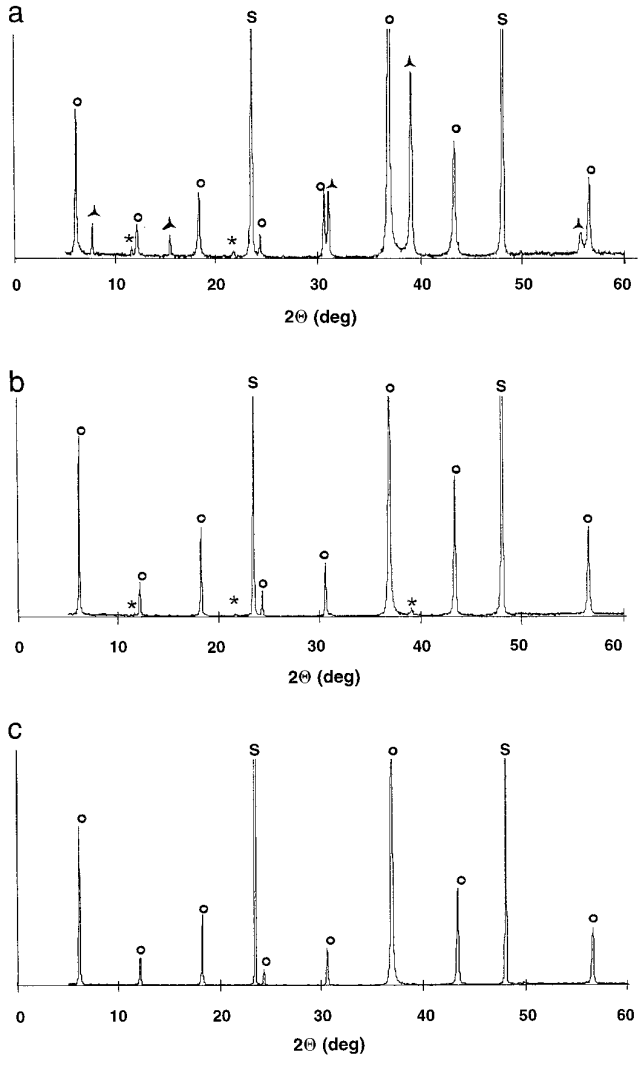

FIG. 11. X-ray diffraction pattern for various annealing times of 2212 precursor film. (a) 0 h, (b) 5 h, (c) 10 h ((S) substrate peaks, (o) 2212 phase, (▲) 2201 phase (*) unknown phase).

suited for the study of the phase changes as a function of annealing time for different starting compositions. Our four target sputtering system allows, by adjusting voltage on the Tl target, the preparation of $Tl_xBa_2CaCu_2O_y$ precursor films with x between 0 and 2. The films are then placed in the high pressure (70 bar) furnace and heated at a rate of 3°C/min (the fastest heating rate achieved by this furnace) up to 880°C and analyzed after different annealing times.

The most important result (Fig. 8) shows that all the films, from the Tl:Ba:Ca:Cu = X:2:1:2 precursor, exhibit, after annealing up to 10 h, the same composition within the experimental errors. But, we must now pay particular attention to the structural analysis by X-ray diffraction. Figures 9, 10, and 11 show, for different X values, the X-ray diffraction patterns corresponding to 0, 5, and 10 h annealing times, respectively. We can see that there is a loss of thallium at the beginning of the annealing for the thallium rich film precursors, but for the Tl:Ba:Ca:Cu = 2:2:1:2 precursor, the film starts to crystallize at the beginning of the annealing and does not contain any other phases after 10 h annealing. This is not the case for the films from Tl:Ba:Ca:Cu = X:2:1:2 precursor, in which, extra phases are not eliminated after 10 h annealing.

DISCUSSION

Since the discovery of Tl-based mixed valence copper oxides, numerous studies have been made to understand the formation of these compounds in thin films. Recently W. Holstein (11) exhaustively reviewed the thermodynamic parameters for the vapor phase processing of Tl-based cuprates superconductors. From this work, it appears that these materials can be understood on the basis of a vapor-solid equilibrium between the volatile species, Tl_2O and O_2, and the Tl–Ba–Ca–Cu–O phases. Gaseous Tl_2O and O_2 are also in equilibrium with solid Tl_2O_3,

$$Tl_2O_3(s) \leftrightarrow Tl_2O(g) + O_2(g), \qquad [1]$$

with an equilibrium constant $K = p(Tl_2O)p(O_2)$. Therefore, it is interesting to know the oxidation state of thallium in the precursor films in order to understand the formation process under high O_2 pressure. We have measured this oxidation state by X-ray absorption spectroscopy (XAS). We have found that thallium is trivalent within the experi-

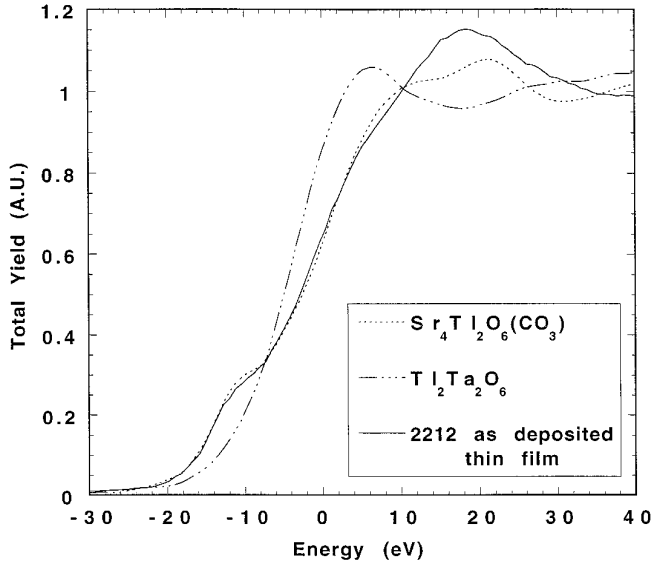

FIG. 12. XAS measurement of an as-deposited 2212 precursor film, compared to reference compound for Tl(I) state and Tl(III) state.

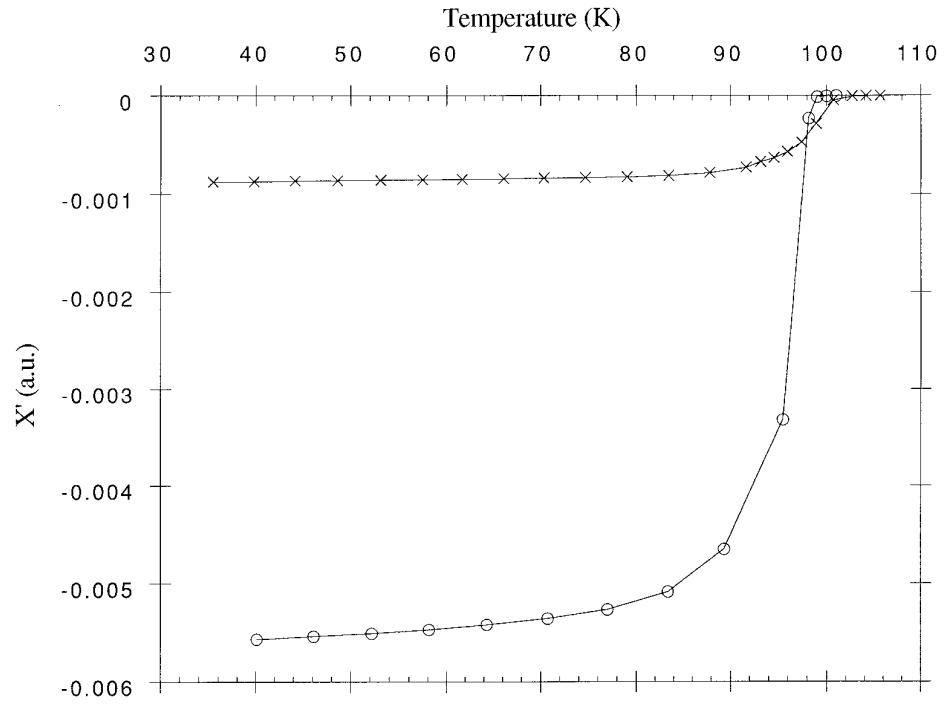

FIG. 13. Diamagnetic transition of a thin film before (o) and after (x) post-annealing under flowing argon at 180°C for 5 min.

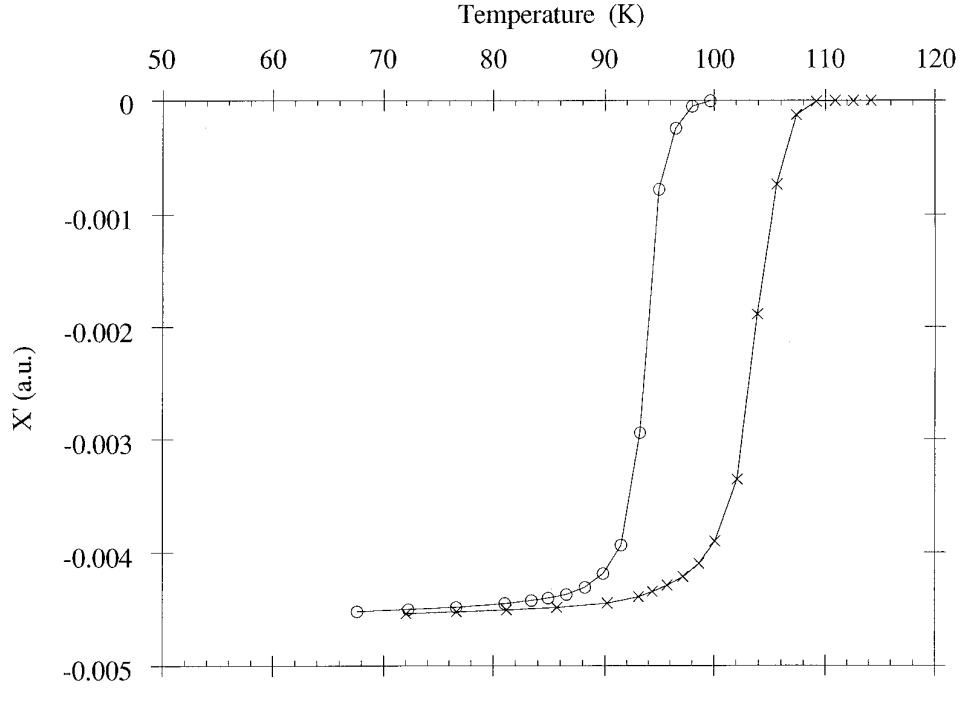

FIG. 14. Diamagnetic transition of a thin film before (o) and after (x) post-annealing under flowing argon/hydrogen at 180°C for 5 min.

mental error (±10% on the mean valence state) by comparing the spectra of thallium in precursor films to those of some reference oxides like $Sr_4Tl_2O_6(CO_3)$ for Tl(III) and $Tl_2Ta_2O_6$ for Tl(I) (Fig. 12) (17, 18).

As all precursor films exhibit the composition BaO : CaO : CuO = 2 : 1 : 2, our work is well described by the thermodynamic relationship published by W. L. Holstein. When annealings occur at high oxygen partial pressure, we can form the 1212 phase which is stable only at high values of $p(O_2)$. The difference in Tl : Ba : Ca : Cu = 2 : 2 : 1 : 2 and Tl : Ba : Ca : Cu = X : 2 : 1 : 2 precursor films arises from the Tl_2O partial pressure. The 2212 films can be synthesized by the reaction

$$2\,BaCuO_2(s) + CaO(s) + Tl_2O(g) + O_2(g) \leftrightarrow Tl_2Ba_2CaCu_2O_8(s) \quad [2]$$

at high $p(Tl_2O)$ and relatively low $p(O_2)$.

At high temperature (>1100 K) the trivalent thallium oxide, which is inside the amorphous precursor, may be decomposed to a mixture of Tl_2O and Tl_4O_3. This decomposition can generate in the film Tl_2O oxide and then induce the above reaction [2] leading to the 2212 formation. A solid state reaction with Tl_2O_3 that leads to the formation of 2212 is possible.

Let us now pay particular attention to the phase diagram of BaO : CaO : CuO = 2 : 1 : 2 published by Holstein (11). The X-ray diffraction pattern (Fig. 11) indicates that only the 2212 precursor films form the intermediate 2201 phase. This fact has no explanation to our knowledge, but seems to be related to a balance between thallium oxide losses and nucleation as discussed further.

The methods of growing the 2212 films are induced by specific reactions during annealing. In the case of annealing in a high pressure furnace (70 bar) the heating rate is low (3°/min). If the film annealing is interrupted at the beginning of the 880°C dwell, the film composition exhibits a thallium deficiency larger than the precursor nonannealed film (for $x > 1$), whereas, the composition of a film grown from the same precursor composition, measured after the 15 h dwell at 880°C is very close to Tl : Ba : Ca : Cu = 2 : 2 : 1 : 2. As a result, with such a heating rate during the first step of the crystallization process, thallium loss for $x > 0.15$ occurs during the increase of the temperature. The second step which takes a longer time is the diffusion of thallium from the gas phase into the film. It is a solid state diffusion mechanism over a long distance which explains why it takes a much longer time. Even if thermodynamics are favorable for the synthesis, the kinetics have some restrictions. If we choose a lower pressure (30 bar), no crystallization is evidenced even after 30 h of annealing. In order to obtain the crystallization of the film, for that pressure, the temperature must be increased to 900°C with a dwell duration of 10 h. Thus to obtain 2212 thallium films from high pressure annealing, a ratio has to be satisfied between pressure and temperature: the higher the pressure is, the lower the temperature must be (the dwell must be shorter, as well).

The annealing in a quartz tube is characterized by a fast heating rate and a sealed tube. Assuming that reaction [1] exhibits slow kinetics, thallium losses must be minimized during the heating of the film. As the thallium atoms stay in the film, the crystallization is faster for this process than in the high pressure furnace.

After complete annealing at high temperature with both methods, attempts were made to optimize the hole carrier density in order to increase T_c. In this case, films are reduced by heating for 5–15 min under argon or hydrogen/argon (10% H_2) for reduction at 200°C. From experimental results it appears that in a hydrogen flow the diamagnetic volume of the films is decreased (Fig. 13), while, in argon we can increase the T_c of films up to 110 K while retaining a sharp transition and a high diamagnetic volume (Fig. 14). This behavior can be compared with that obtained in bulk materials (19) in which oxygen concentration can be controlled with a post-annealing treatment at 280°C. The problem of the doping hole concentration will be addressed by XAS in a future paper (20).

CONCLUSION

The 2212 thallium films can be crystallized from amorphous precursor films with variable thallium content prepared by a sputtering process. This process appears to be a well-adapted method to obtain films on large surfaces (about 5 cm) with high T_c and J_c. We have checked two different ways of annealing which involve different precursor films. It appears from our study that the crystallization of amorphous Tl : Ba : Ca : Cu = 2 : 2 : 1 : 2 precursor films having a stoichiometric thallium content is a route to prepare good films under high oxygen pressure. In the same way, in sealed tubes it is possible to obtain a single phase, highly oriented film with a good surface when Tl : Ba : Ca : Cu = 2 : 2 : 1 : 2 precursor films are annealed in medium oxygen pressure.

ACKNOWLEDGMENTS

We express our gratitude to the team of the Van de Graff of the CENBG for having the opportunity to make the measurements with the nuclear microprobe, especially Y. Labrador for his kind and constant assistance, and to S. Flament (GREYC, ISMRA Caen, France) for critical current measurement.

REFERENCES

1. Z. Z. Sheng, A. M. Hermann, A. El Ali, C. Almason, J. Estrada, T. Datta, and R. J. Matson, *Phys. Rev. Lett.* **60,** 937 (1988).

2. D. Miller, P. L. Richards, S. M. Garrison, N. Newman, C. B. Eom, T. H. Geballe, S. Etamad, A. Inam, T. Venkatesan, J. S. Martens, N. Y. Lee, and L. C. Bourne, *J. Supercond.* **5**(4), 379 (1992).
3. S. H. Liou, K. D. Aylesworth, N. J. Ianno, B. Johs, D. Thompson, D. Meyer, J. A. Woollham, and C. Barry, *Appl. Phys. Lett.* **54**(8), 760 (1989).
4. M. Hong, S. H. Liou, D. D. Bacon, G. S. Grader, J. Kwo, R. R. Kortan, and B. A. Davidson, *Appl. Phys. Lett.* **53**(21), 2102 (1988).
5. J. H. Kang, K. E. Gray, R. T. Kampwirth, and D. W. Day, *Appl. Phys. Lett.* **53**(25), 2560 (1988).
6. D. G. Naugle and P. S. Wang, *Mater. Sci. Eng. A* **134,** 1251 (1991).
7. D. S. Richeson, L. M. Tonge, J. Zhao, J. Zhang, H. O. Marcy, T. J. Marks, B. W. Wessels, and C. R. Kannewurf, *Appl. Phys. Lett.* **54**(21), 2154 (1989).
8. D. W. Face and J. P. Nestlerode, *Appl. Phys. Lett.* **61**(15), 1838 (1992).
9. W. L. Holstein, *J. Phys. Chem.* **97,** 4224 (1993).
10. M. Lanham, T. W. James, M. Eddy, F. F. Lange, and D. R. Clarke, *Appl. Phys. Lett.* **62**(23), 3028 (1993).
11. W. L. Holstein, *Appl. Supercond.* **2**(5), 345 (1994).
12. L. Coudrier, B. Mercey, and H. Murray, *Supercond. Sci. Technol.* **6,** 119 (1993).
13. C. Prouteau, J. F. Hamet, B. Mercey, M. Hervieu, B. Raveau, D. Robbes, L. Coudrier, and G. Benassayag, *Physica C* **248,** 108 (1995).
14. M. Fendrof, M. Powers, and R. Gronsky, *Microsc. Res. Tech.* **30,** 167 (1995).
15. L. R. Doolittle, *Nucl. Instrum. Meth. B* **9,** 344 (1985).
16. W. L. Holstein, L. A. Parisi, R. B. Flippen, and D. G. Swartzfager, *J. Mater. Res.* **8**(5), 962 (1993).
17. F. Studer, D. Bourgault, C. Martin, R. Retoux, C. Michel, and B. Raveau, *Physica C* **159,** 609 (1989).
18. F. Studer, N. Merrien, C. Martin, C. Michel, and B. Raveau, *Physica C* **178,** 324 (1991).
19. C. Martin, A. Maignan, J. Provost, C. Michel, M. Hervieu, R. Tournier, and B. Raveau, *Physica C* **168,** 8 (1990).
20. C. Gasser, F. Studer, A. Maignan, H. Murray, to be published.